**Eleventh U.S. National Conference on Earthquake Engineering**
*Integrating Science, Engineering & Policy*
June 25-29, 2018
Los Angeles, California

# VISUALIZING THE DEMAND AND CAPACITY FACTOR DESIGN (DCFD) FORMAT FOR SAFETY-CHECKING

F. Jalayer[1]

**ABSTRACT**

Demand and capacity factor design (DCFD), which forms the analytical backbone of probabilistic performance evaluation in FEMA 350, essentially consists of a closed-form and analytical expression for the mean annual rate of exceeding a prescribed performance level. The format has been widely used, due to both its utility and simplicity of formulation. The DCFD has often tempted the researchers into trying to overcome its potential inaccuracies due to the underlying simplifying assumptions. The assumptions of a power-law hazard curve and Lognormality of the engineering demand parameter (EDP) given the intensity measure (IM) are distinguished as the two main causes of the inaccuracies in the formulation. This work offers an alternative glance into the original DCFD safety-checking format as a visual safety-checking instrument. The visualization draws upon overlapping of fragility and hazard curves. One of the advantages offered by this graphical procedure is that the site-specific hazard curve can be employed and visualized directly (only a slope parameter needs to be estimated). The proposed framework employs a reliability-based critical demand to capacity ratio as a global performance variable. It is shown that the proposed visual DCFD procedure leads –within acceptable limits of accuracy—to results that are comparable with those obtained through a direct calculation of risk by employing numerical integration, for the case-study frame and the collapse prevention performance level.

[1]Associate Professor, Dept. of Structures for Engineering and Architecture, University of Naples Federico II, Naples, Italy 80125 (email: fatemeh.jalayer@unina.it)

Jalayer F. Visualizing the Demand and Capacity Factor Design (DCFD) format for safety-checking. *Proceedings of the 11th National Conference in Earthquake Engineering*, Earthquake Engineering Research Institute, Los Angeles, CA. 2018.

# Visualizing the Demand and Capacity Factor Design (DCFD) format for safety-checking

F. Jalayer[1]

**ABSTRACT**

Demand and capacity factor design (DCFD), which forms the analytical backbone of probabilistic performance evaluation in FEMA 350, essentially consists of a closed-form and analytical expression for the mean annual rate of exceeding a prescribed performance level. The format has been widely used, due to both its utility and simplicity of formulation. The DCFD has often tempted the researchers into trying to overcome its potential inaccuracies due to the underlying simplifying assumptions. The assumptions of a power-law hazard curve and Lognormality of the engineering demand parameter (EDP) given the intensity measure (IM) are distinguished as the two main causes of the inaccuracies in the formulation. This work offers an alternative glance into the original DCFD safety-checking format as a visual safety-checking instrument. The visualization draws upon overlapping of fragility and hazard curves. One of the advantages offered by this graphical procedure is that the site-specific hazard curve can be employed and visualized directly (only a slope parameter needs to be estimated). The proposed framework employs a reliability-based critical demand to capacity ratio as a global performance variable. It is shown that the proposed visual DCFD procedure leads –within acceptable limits of accuracy—to results that are comparable with those obtained through a direct calculation of risk by employing numerical integration, for the case-study frame and the collapse prevention performance level.

## Introduction

Demand and capacity factor design (DCFD, [1,2,3]), which forms the analytical backbone of probabilistic performance evaluation in FEMA 350 [4], is consisted of (the rearrangement of) a closed-form and analytical expression for the mean annual rate of exceeding a prescribed performance level. The format has been widely used, due to both its utility and simplicity of formulation. It has also been closely analyzed and criticized for its potential to lead to inaccurate performance evaluation [5-10]. However, albeit often valid allegations of inaccuracy, it has never ceased to fascinate the researchers and to challenge them into modifying it to overcome some of the causes of such inaccuracies. For the most part, the assumption of a power-law hazard curve (with a constant logarithmic slope) and the assumption of the Lognormality (power-law median with a constant logarithmic standard deviation) of the engineering demand parameter (EDP) given the intensity measure (IM) are recognized as the two main causes of the inaccuracies in the formulation, with the first one being much more important. However,

[1] Associate Professor, Dept. of Structures for Engineering and Architecture, University of Naples Federico II, Naples, Italy 80125 (email: fatemeh.jalayer@unina.it)

Jalayer F. Visualizing the Demand and Capacity Factor Design (DCFD) format for safety-checking. Proceedings of the 11th National Conference in Earthquake Engineering, Earthquake Engineering Research Institute, Los Angeles, CA. 2018.

improving DCFD has proved to be very challenging as any effort to overcome and relax some of its underlying assumptions risks to further complicate its attractive back-of-the-envelope formulation. The current work offers a glance into the DCFD safety-checking format as a visual and practical instrument for controlling whether the structure manages to verify the performance level of interest. The visualization basically draws upon the overlapping of fragility and hazard curves. To achieve such graphical visualization, an (intensity measure) IM-based version of the format is adopted (developed in [2]) which compares factored demand defined in terms of the intensity measure that corresponds to a given hazard level (set numerically equal to the allowable risk level) and the factored capacity defined in IM terms. One of the most useful advantages offered by this graphical procedure is that the site-specific hazard curve can be employed and visualized directly. A major twist in the proposed formulation involves the choice of the engineering demand parameter (EDP) and the structural capacity. The proposed framework adopts a global performance variable expressed in demand-to-capacity ratio terms for the structure. The critical demand to capacity ratio is defined for a prescribed performance level and is –by definition- equal to unity at the onset of the limit state. Therefore, the factored capacity is defined in terms of the intensity measure that corresponds to the onset of limit state or the critical demand to capacity equal to unity and can be derived based on the information provided by the fragility curve; that is, the median IM corresponding to the onset of the performance level (a.k.a., median IM capacity) and its logarithmic standard deviation. It is worth mentioning that even if the fragility curve turns out to be not Lognormal, this visual procedure can extract the equivalent Lognormal statistics. In this approach the slope of the hazard curve is estimated as the slope of the hazard curve at the median IM capacity as suggested in [3]. This is, the point on the hazard curve which is going to receive the largest weight from the fragility in the risk integral. It is also shown (through an illustrative example) that the proposed visual DCFD procedure leads –within acceptable limits of accuracy—to results that are comparable with those obtained through a direct calculation of risk by employing numerical integration.

## The Performance Parameter

One of the main characteristics of a safety-checking format like DCFD is that it adopts a scalar parameter to represent the global performance of a building. Naturally, the format can assume several alternative formulations based on the choice of such scalar parameters. The DCFD has been used most often by adopting the maximum inter-story drift as the engineering demand parameter. In such context, the structural demand and capacity are expressed in terms of the maximum inter-story drift ratio. Alternatively, the DCFD format can be adapted so that the performance parameter is the intensity value that corresponds to the onset of the performance level. This latter interpretation is known as the IM-based version [2]. Herein, a normalized performance variable denoted as $DCR_{\mathrm{pl}}$ is employed [11-13] which is defined as the critical demand to capacity ratio for the structure. The main point about this performance variable is that it is, by definition, equal to unity at the onset of the performance level. For instance, the DCFD format based on the maximum inter-story drift ratio can be easily transformed into a demand to capacity ratio form by normalizing the maximum inter-story drift demand to maximum inter-story capacity. It is to note that this representation of the performance variable can automatically consider the possible correlations between seismic demand and capacity. Naturally, the IM-based version of the DCFD format is going to be based on the IM value that corresponds to the onset of performance level marked as $DCR_{\mathrm{pl}}=1$.

## Demand and Capacity Factor Design (IM-based version)

The demand and capacity factor design [1-3] is a closed-form and analytical format derived for probabilistic performance-based seismic safety checking. Being formulated in an LRFD-like manner, it compares the seismic demand and capacity in probabilistic terms: the seismic demand is increased to account for the uncertainty in predicting the demand for an acceptable risk level and the seismic capacity is decreased to consider the uncertainty in predicting the seismic capacity for a given performance level (or limit state). This probabilistic safety-checking format is based on rigorous probabilistic principles. However, the probabilistic basis is well-disguised through rearrangement in terms of the engineering demand parameter (EDP) or alternatively in terms of the intensity measure (IM). More specifically, the format generates from the risk-based statement of the performance objective for a prescribed performance level:

$$\lambda_{pl} \le P_o \qquad (1)$$

Where $\lambda_{pl}$ is the seismic risk expressed in terms of the mean annual frequency of exceeding a specific performance level *pl* and $P_o$ is an acceptable risk level (e.g., 5% in 50 years for the Collapse Prevention performance level [14], see Fig. 1b).

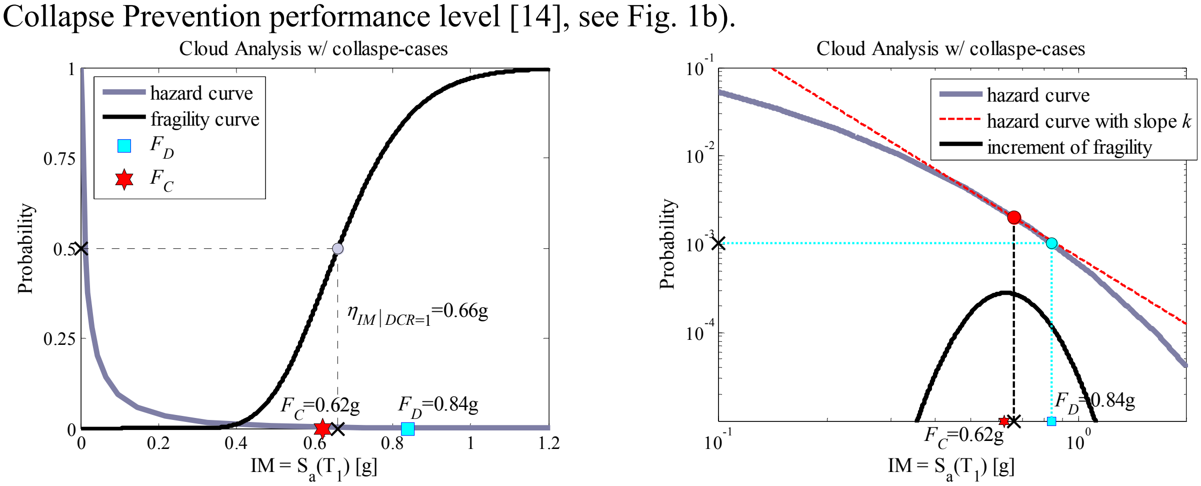


Figure 1. The IM-based version of the DCFD safety-checking format: the main players (a) the visual fragility/hazard representation; (b) the estimation of the slope *k*

The DCFD safety checking format is derived into closed- and analytical form by making a series of assumptions: (1) the performance level exceedance can be expressed as a homogenous Poisson process; (2) the *hazard curve* (the mean annual frequency of exceeding a given seismic intensity level) denoted as $\lambda_{IM}$ is approximated by a power-law curve of the form $\lambda_{IM} = k_o IM^k$; (3) the IM capacity is expressed as a Lognormal distribution with median $\eta_{IM|DCR=1}$ and logarithmic standard deviation $\beta_{IM|DCR=1}$. The IM-based representation of the DCFD (neglecting the epistemic uncertainties) is expressed as:

$$FD = IM_{P_o} \le FC = \eta_{IM|DCR=1} \cdot \phi \qquad (2)$$

Where FD the factored demand is equal to $IM_{P_o}$ which (as illustrated in Fig. 1b) is the intensity measure corresponding to the acceptable risk level $P_o$ through the hazard curve; $\eta_{IM|DCR=1}$ is the median seismic intensity at the onset of the performance level *pl* (described in more detail in the next section); $\phi$ is a de-magnifying factor applied to seismic capacity and is expressed as:

$$\phi = \exp\left( -\frac{k}{2} \beta_{IM|DCR=1}{}^{2} \right) \tag{4}$$

Where $\beta_{\mathrm{DCR|IM}}$ is the logarithmic standard deviation (i.e., the standard deviation of the logarithm) of the seismic intensity IM at the onset of the performance level (note that the subscript *pl* of the demand to capcity ratio is dropped for the sake of brevity of notation). The next section describes in detail how $\beta_{\mathrm{IM|DCR=1}}$ and $\eta_{IM|DCR=1}$ can be estimated.

One very important and decisive factor for the accuracy of the DCFD safety-checking format is the estimation of the slope parameter *k*. The risk integral (for calculating $\lambda_{pl}$ accurately) can be calculated numerically as the area under the risk integrand. This latter for each IM value is equal to the product of hazard curve and the fragility increment (i.e., probability density function PDF of the IM capacity times the integration IM step). Therefore, the fragility increment can be viewed (for risk assessment) as the values used for weighting the hazard curve (the thick solid bell-shaped curve Fig. 1b). It can be shown that for a Lognormal fragility curve the fragility increment is a maximum at median IM capacity value $\eta_{IM|DCR=1}$ and will become negligible at the two extremes of the fragility curve. Therefore, it is expected that the vicinity of the $\eta_{IM|DCR=1}$ is the most important area to be captured by the approximate hazard line in the log-log scale (the red dashed line in Fig 1b). Herein, the slope of the hazard curve is estimated as the slope of the tangent line illustrated in Fig.1b in the log-log scale. The Fig. 1b also shows the procedure for finding the FD=$IM_{\mathrm{Po}}$ (since the probability level $P_{\mathrm{o}}$ is small, it cannot be viewed properly in Fig. 1a which is in arithmetic scale.)

## Nonlinear Dynamic Analysis Methods for Implementation in DCFD

To visualize the seismic capacity in the IM-based DCFD format, the compatible IM-based interpretation of the fragility curve is particularly useful (see e.g., [15]). This interpretation expresses the seismic fragility as the cumulative distribution for the capacity expressed in IM terms; in other words, the intensity value that corresponds to the onset of performance level $\mathrm{IM_{pl}}$:

$$P(pl \mid IM) = P(IM_{pl} \le IM) = \Phi\left( \frac{\ln\left( IM / \eta_{IM|DCR=1} \right)}{\beta_{IM|DCR=1}} \right) \tag{5}$$

In this section some alternative non-linear dynamic analysis methods are applied in order estimate the median $\eta_{\mathrm{IM|DCR=1}}$ and the logarithmic standard deviation $\beta_{\mathrm{IM|DCR=1}}$ for $IM_{\mathrm{pl}}$.

### From the simple Cloud Analysis

The Cloud Analysis ([1,3,12,13]) is a non-linear dynamic analysis procedure that is most often applied to structural response to as-recorded (un-scaled) ground motion time-histories. The Cloud Analysis is the default method for implementation of main DCFD format (a.k.a, the EDP-based version) as it is perfectly compatible with its underlying assumptions. More specifically, the median performance variable $DCR_{\mathrm{pl}}$ for the prescribed performance level *pl* is described as a power-law function of the seismic intensity level:

$$DCR_{pl} = a \cdot IM^{b} \tag{5}$$

This is equivalent to a linear regression model in the logarithmic scale. Moreover, it is assumed that the logarithmic standard deviation in the performance variable $DCR_{pl}$ given seismic intensity and denoted as $\beta_{DCR|IM}$ is invariable with respect to the intensity level (equivalent to the assumption of a homoscedastic regression). Moreover, it is assumed that the performance variable given the intensity level can be described by a Lognormal probability model. Fig. 2a illustrates the performance variable $DCR_{pl}$ and intensity (herein, the first mode spectral acceleration) pairs ($DCR_{pl,i}$ , $IM_i$), $i$=1:$N$ obtained in response to a suite of $N$ ground motion records. The figure also illustrates the power-law curve fitted to the data points. The median intensity level $\eta_{IM|DCR=1}$ corresponding to the onset of limit state can be estimated as the point on the power-law curve that corresponds to the onset of limit state; that is $(1/a)^{1/b}$. $\beta_{IM|DCR=1}$ can be estimated as a function of the standard error of the regression:

$$\beta_{IM|DCR=1} = \frac{1}{b}\sqrt{\frac{\sum_{i=1}^{N}\left(\ln\left(\frac{DCR_{pl,i}}{a \cdot IM_i^{\,b}}\right)\right)^2}{N-2}} \tag{6}$$

Note that the standard deviation $\beta_{IM|DCR=1}$ is calculated as $\beta_{DCR|IM}/b$ where $\beta_{DCR|IM}$ is the standard error of regression.

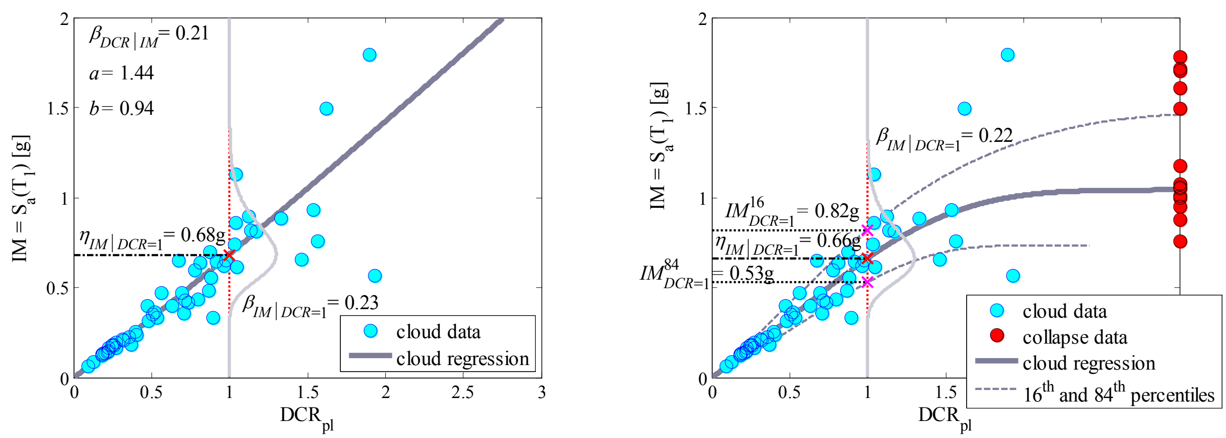


Figure 2 (a) The simple Cloud Analysis; (b) Cloud Analysis considering the collapse cases

**From Cloud Analysis considering the collapse cases**

Jalayer et al. [13] have demonstrated that the Cloud Analysis can lead to sufficiently accurate results if the ground motion records are selected so that they can populate both sides of $DCR_{pl}$ =1. For ultimate performance levels such as *life safety* and *collapse prevention*, this may lead to numerical non-convergence and/or global dynamic instability –generically referred to as the "collapse cases". Shome and Cornell [5] proposed a modified version of the DCFD format in which the "collapse cases" where considered explicitly. This has inspired the proposal of a modified version of the Cloud Analysis in [13], in which the simple Cloud Analysis as described in the previous paragraph is applied to the non-collapse-inducing records and the collapse-inducing records are treated separately. This leads to a non-Lognormal description of the structural fragility expressed as a weighted average of the (two-parameter) Lognormal cumulative distribution describing the non-collapse-inducing records and unity. The weights (which sum to unity) are the probability of non-collapse given the intensity level denoted as $P(NoC|IM)$ and the probability of collapse given the intensity level denoted as $P(C|IM)$. In the original version presented by Shome and Cornell [5], the probability of collapse $P(C|IM)$ was estimated as the ratio of the number of collapse-inducing records to the total number of records. In the modified version of the Cloud Analysis considering the collapse cases proposed in [13], the probability of collapse given the intensity level is estimated by a bi-parametric logistic regression. It is interesting to note that the $p^{th}$ percentile of the performance variable given IM can be expressed as:

$$DCR^{p}(IM) = DCR_{NoC}(IM) \cdot \exp\left(\beta_{DCR|IM,NoC} \cdot \Phi^{-1}\left[p/P(NoC\,|\,IM)\right]\right) \quad (7)$$

where $DCR^{p}$ is the $p^{th}$ percentile of the performance variable as a function of the seismic intensity, $DCR_{NoC}(IM)=aIM^{b}$ is the median performance variable for the non-collapse portion of the data as a function of the seismic intensity and $\Phi^{-1}$ is the inverse function of standardized normal distribution. Fig. 2b illustrates another example of Cloud data pairs where collapse cases are identified. The $16^{th}$ percentile ($p$=0.16), median ($p$=0.50) and $84^{th}$ percentile ($p$=0.84) curves obtained from Eq. 7 are also illustrated in Fig. 2b. The median intensity at the onset of the performance level $\eta_{IM|DCR=1}$ can be obtained by finding the intensity value corresponding to unity from the median performance curve. The $\beta_{IM|DCR=1}$ can be estimated as half of the logarithmic (vertical) distance between the $16^{th}$ and the $84^{th}$ percentile curves measured at $DCR_{pl}$ =1; that is: $0.5\ln(IM_{pl}^{16}/IM_{pl}^{84})$ in Fig. 2b.

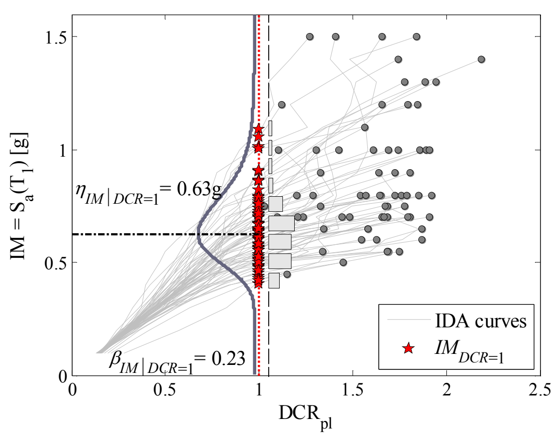


Figure 3. The incremental dynamic analysis and the distribution of IM capacities

## From the IDA Analysis

The incremental dynamic analysis [16] is a non-linear dynamic analysis method in which a suite of ground motion records are scaled linearly in amplitude in order to obtain a set of IDA curves. The IDA analysis lends itself quite well to the IM-based interpretation of the DCFD format. Figure 4 demonstrates the IDA curves derived for a suite of ground motion records. The figure also shows the median IDA curve. The $IM_{pl,i}$ , ($i$=1:$N$) which are the seismic intensity values that correspond to the onset of the performance level ($DCR_{pl}$ =1) for each of the $N$ IDA curves, are also illustrated in the figure. Fig. 3 shows a Lognormal curve fitted to these $IM_{pl,i}$ points. The

$\eta_{IM|DCR=1}$ value can be estimated as the median of this Lognormal distribution. The $\beta_{IM|DCR=1}$ can be estimated as the logarithmic standard deviation of the $IM_{pl,i}$ points.

## The numerical Example

One of the transverse frames of the seven-story hotel building in Van Nuys, California, is modeled and analyzed in this study (Fig. 4). The building is in the San Fernando Valley of Los Angeles County (34.221° north latitude, 118.471° west longitude). The frame building was constructed in 1966 according to the 1964 Los Angeles City Building Code. The building was damaged in the M6.7 1994 Northridge earthquake. After the 1994 earthquake, the building was retrofitted with addition of new RC shear walls. The original building (in its pre-retrofit condition) is modeled herein (see Miano et al. [17] for more details). The flexural-axial behavior is modelled using the fiber section (30 uniaxial fiber layers adopting OPENSEES Concrete01 and Steel02 Giuffré-Pinto-Meneghotto strain-hardening in steel) with distributed plasticity (five-point Newton-Cotes Integration) for the columns and concentrated plasticity for the beams (modified Gauss-Radau integration). The shear behavior is modeled as a non-linear and degrading translational zero-length spring in the top of the column up to the point of axial failure. The rigid end rotation due to bar-slip is modeled through two zero-length rotational springs at the two ends of the column members [18].

A set of 70 strong ground-motion records are selected from the NGA-West2 database [19] (see [13] for the list of records). This suite of records covers a wide range of magnitudes between 5.5 and 7.9, and closest distance-to-ruptured area up to around 40 km. The soil average shear wave velocity in upper 30 m of soil, Vs30, at the site is around 218 m/sec. Accordingly, all selected records are chosen from NEHRP site classes C-D. A limit of maximum six recordings from a single seismic event has been considered (except for Loma Prieta event from which 8 events are chosen). Moreover, only one of the two horizontal components of each recording, the one with larger spectral acceleration at 1.0 sec is selected (fundamental period $T_1$=1.11). The lowest useable frequency is set at 0.25 Hz. The records are from strike-slip or reverse faults (consistent with California faulting); They are either free field or on the ground level. Finally, there are no specific considerations for spectral shape, epsilon, and no distinction is made between the wave-forms in terms of ordinary and pulse-like ground motions.

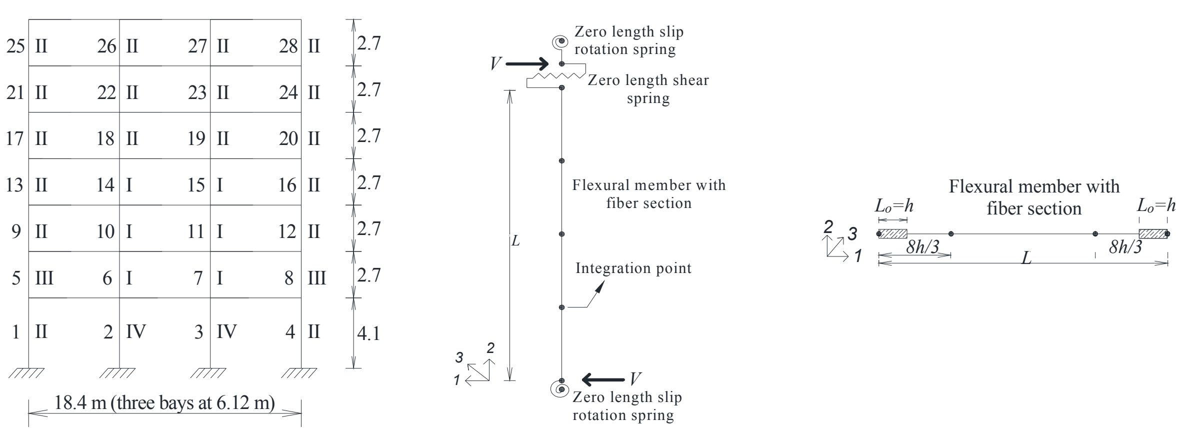


Figure 4 The moment-resisting frame and the finite element model for columns and beams

First-mode spectral acceleration is chosen as the intensity measure. Being a regular moment-resisting frame of medium height, it is expected that the first-mode spectral acceleration is relatively sufficient with respect to ground motion characteristics ([3,20]). The structure is to be assessed for the performance level of collapse prevention [14] based on an enhanced performance objective with $P_o$=0.001. It has been made sure that the $DCR_{\text{pl}}$ values for the collapse prevention populate also the greater than unity zone. The mean site-specific hazard curve is calculated at T=1 sec and is extracted from USGS National Seismic Hazard Mapping Project website (http://earthquake.usgs.gov/hazards, last accessed Nov. 2017). The performance variable $DCR_{\text{pl}}$ is adopted as the demand to capacity ratio that brings the structure closest to the onset of the performance level (see [13] for more detail). The $DCR_{\text{pl}}$ is calculated as the maximum demand to capacity chord rotation ratio for all the elements of the frame. The collapse-inducing records are distinguished (according to [21]) as those records for which (a) 50%+1 of the columns in only one story reach the chord rotation corresponding to the the complete loss of vertical-load carrying capacity; (b) the maximum inter-story drift exceeds 10% (to account for global dynamic instability).

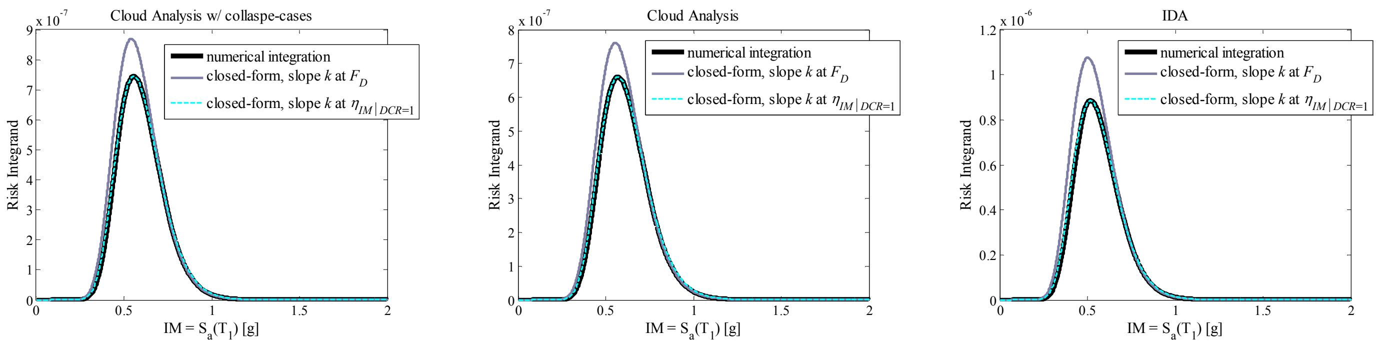


Figure 5 The risk integrand for the three considered non-linear dynamic analysis procedures (a) Cloud with collapse cases; (b) Cloud Analysis; (c) IDA

## Application of the DCFD Procedure

The IM-based version of the DCFD format is applied herein for safety-checking of the case-study frame for the Collapse Prevention performance level. The factored demand is calculated as the spectral acceleration value corresponding to the $P_{\text{o}}$=0.001 (see Fig. 1a) from the site-specific hazard curve calculated for a period ($T$=1s) close to the fundamental period of the structure ($T_1$=1.11s). Fig. 1a illustrates the visual DCFD procedure for Cloud Analysis with collapse cases. However, the procedure for determining the FD is the analogous for all the three non-linear dynamic analysis methods discussed above (reported in Table 1). The three methods distinguish themselves in the way in which they estimate the median and the logarithmic standard deviation for the IM capacity (IM corresponding to the onset of the performance level $DCR_{\text{pl}}$) to be replaced in Eq. 5. It is interesting to note that the parameters necessary for calculating the factored capacity FC can be all extracted visually from the fragility curve (for example the fragility shown in Fig.1a). The median for the IM capacity $\eta_{\text{IM|DCR=1}}$ is the IM value corresponding to the 50% probability level. The logarithmic standard deviation $\beta_{\text{IM|DCR=1}}$ can be estimated as half of the distance in logarithmic scale between the IM values corresponding to 84% and 16% probability levels. This can be useful for estimating the equivalent Lognormal $\eta_{\text{IM|DCR=1}}$ and $\beta_{\text{IM|DCR=1}}$ values for non-Lognormal fragility curves (here, these statistics are calculated according to the procedures described above and not visually). The $k$ parameter is estimated (as illustrated in Fig 1b) for each non-linear dynamic analysis method as the slope of the tangent line (in the log-log scale) to the hazard curve at the IM capacity $\eta_{IM|DCR=1}$.

Table 1. The comparison between numerical integration and the DCFD safety-checking

| **Analysis Type** | $\lambda_{NI}$ | $\lambda_{Closed\text{-}Form}$ | $F_D$ [g] | $F_C$ [g] | $F_D$ / $F_C$ | $\lambda_{NI}$ / $P_o$ | $\lambda_{Closed\text{-}Form}$ / $P_o$ |
|---|---|---|---|---|---|---|---|
| IDA | 0.0027 | 0.0027 | 0.84 | 0.58 | 1.43 | 2.60 | 2.67 |
| Cloud Analysis | 0.0021 | 0.0022 | 0.84 | 0.64 | 1.31 | 2.09 | 2.13 |
| Cloud w/ collapse | 0.0023 | 0.0024 | 0.84 | 0.62 | 1.35 | 2.25 | 2.29 |

Figures 5a,b,c show the risk integrands calculated for all the three methods (Cloud with collapse cases, Cloud and IDA) based on numerical integration and based on DCFD-based assumptions. The figures show that the DCFD leads to almost exact results for all three cases. Table 1 tabulates the risk calculations (both numerical integration and based on DCFD assumptions), the factored demand and the factored capacity for all the three analysis procedures considered. It is to underline that the only approximation in the DCFD results (with respect to the exact numerical integration) in the cases presented in this paper is in the estimation of the factored demand and slope $k$. As it can be seen from Fig. 1b, the tangent line at the median capacity manages to provide exact results in the zone which is going to be weighted the most by the fragility increment.

## Conclusions

The IM-based version of the Demand to Capacity Factored Design (DCFD) format lends itself quite well to a visual fragility/hazard interpretation and reduces to a minimum the underlying assumptions necessary for deriving a simple closed-form. The fragility curve in this context can be calculated based the IM-based interpretation in which fragility is the cumulative distribution of the IM capacity. This IM-based interpretation has the advantage of relaxing the assumptions regarding the linear regression of engineering demand parameter versus IM (the power-law assumption and the homoscedasticity). Consequently, the slope factor $b$ (i.e., slope of the EDP-IM curve in the logarithmic scale) also disappears from the format's closed-from. The only approximations involved in DCFD's closed form are going to be related to the estimation of the factored demand and the slope parameter $k$. It is shown that the best-estimate for slope $k$ is obtained as the slope of the line tangent to the hazard curve in the logarithmic scale at the median IM capacity (as the point which is weighted the most by the fragility increment in the risk integral). Finally, adopting as the performance parameter a global demand to capacity ratio (instead of maximum inter-story drift), facilitates to a great deal the identification of the IM values at the onset of the performance level (the performance variable is equal to unity at the onset of the performance level). This also considers in an automatic manner the possible correlations between seismic demand and seismic capacity.

## Acknowledgements

This work is supported in part by the executive Project ReLUIS-DPC 2014/2018. The author would like to gratefully acknowledge Dr. Hossein Ebrahimian and Ph.D. candidate Andrea Miano for their invaluable help and support with the case-study demonstration.

## References


1. Cornell CA, Jalayer F, Hamburger RO, FAZ<outch DA. Probabilistic basis for 2000 SAC federal emergency management agency steel moment frame guidelines. *Journal of Structural Engineering (ASCE)* 2002; **128** (4): 526-533.
2. Jalayer F, Cornell CA. A Technical Framework for Probability-Based Demand and Capacity Factor Design (DCFD) Seismic Formats**.** *Pacific Earthquake Engineering Center* (*PEER*) **2003/08.**
3. Jalayer F. *Direct probabilistic seismic analysis: implementing non-linear dynamic assessments*. PhD Dissertation, Department of Civil and Environmental Engineering, Stanford University: Stanford, CA, 2003.
4. FEMA-350 *Recommended Seismic Design Criteria for New Steel Moment-Frame Buildings*. Federal Emergency Management Agency: Washington, DC, 2000.
5. Shome N, Cornell CA. Probabilistic seismic demand analysis of nonlinear structures. Report No. RMS35, Stanford University, CA, 1999: 320 pp.
6. Aslani H, Miranda E. Probability-based seismic response analysis. *Eng. Struct.* 2005; **27**(8): 1151-1163.
7. Dolsek M, Fajfar P. The effect of masonry infills on the seismic response of a four storey reinforced concrete frame—a probabilistic assessment. *Engineering Structures* 2008; **30**(11):3186–3192.
8. Bradley BA, Dhakal RP. Error estimation of closed-form solution for annual rate of structural collapse. *Earthquake Engineering and Structural Dynamics* 2008; **37**(15):1721-1737.
9. Vamvatsikos D. Accurate Application and Second-Order Improvement of SAC/FEMA Probabilistic Formats for Seismic Performance Assessment. *Journal of Structural Engineering* 2014; **140**(2).
10. Vamvatsikos D. Derivation of new SAC/FEMA performance evaluation solutions with second-order hazard approximation. *Earthquake Engineering and Structural Dynamics* 2013, **42**(8), 1171–1188.
11. Jalayer F, Franchin P, Pinto PE. A scalar damage measure for seismic reliability analysis of RC frames. *Earthquake Engineering and Structural Dynamics* 2007; **36** (13): 2059–2079.
12. Jalayer F, De Risi R, Manfredi G. Bayesian Cloud Analysis: efficient structural fragility assessment using linear regression. *Bulletin of Earthquake Engineering* 2015; **13** (4): 1183-1203.
13. Jalayer F, Ebrahimian H, Miano A, Manfredi G, Sezen H. Analytical fragility assessment using un-scaled ground motion records. *Earthquake Engineering and Structural Dynamics* 2017; 46 (15): 2639-2663.
14. ASCE/SEI 41-13. *Seismic Evaluation and Retrofit of Existing Buildings*. American Society of Civil Engineers: Reston, VA, 2014.
15. Eads L, Miranda E, Lignos DG. Average spectral acceleration as an intensity measure for collapse risk assessment. *Earthquake Engineering and Structural Dynamics* 2015; **44** (12): 2057-2073.
16. Vamvatsikos D, Cornell CA. Incremental dynamic analysis. *Earthquake Engineering and Structural Dynamics* 2002; **31** (3): 491-514.
17. Miano A, Sezen H, Jalayer F, Prota A. Performance based comparison of different retrofit methods for reinforced concrete structures. In: *Proceedings of the 6$^{th}$ ECCOMAS Thematic Conference on Computational Methods in Structural Dynamics and Earthquake Engineering (COMPDYN 2017)*, Rhodes, Greece, 15-17 June 2017.
18. Setzler EJ, Sezen H. Model for the lateral behavior of reinforced concrete columns including shear deformations. *Earthq Spectra*. 2008; **24**(2): 493-511.
19. Ancheta TD, et al. NGA-West2 Database. *Earthquake Spectra* 2014; **30**(3), 989-1005.
20. Jalayer F, Beck J, Zareian F. Analyzing the sufficiency of alternative scalar and vector intensity measures of ground shaking based on information theory. *Journal of Engineering Mechanics* 2012; **138** (3): 307-316.
21. Galanis PH, Moehle JP. Development of collapse indicators for risk assessment of older-type reinforced concrete buildings. *Earthquake Spectra* 2015; **31** (4): 1991-2006.